



Published in final edited form as:

*Neuropsychologia*. 2015 July ; 73: 12–24. doi:10.1016/j.neuropsychologia.2015.04.032.

## Intraparietal regions play a material general role in working memory: evidence supporting an internal attentional role

Kyle Killebrew<sup>1</sup>, Ryan Mruzek<sup>1,2</sup>, and Marian E. Berryhill<sup>1</sup>

<sup>1</sup>University of Nevada, Reno, NV 89557

<sup>2</sup>Worcester State University, Worcester, MA 01602

### Abstract

Determining the role of intraparietal sulcus (IPS) regions in working memory (WM) remains a topic of considerable interest and lack of clarity. One group of hypotheses, the internal attention view, proposes that the IPS plays a material general role in maintaining information in WM. An alternative viewpoint, the pure storage account, proposes that the IPS in each hemisphere maintains material specific (e.g., left – phonological; right – visuospatial) information. Yet, adjudication between competing theoretical perspectives is complicated by divergent findings from different methodologies and their use of different paradigms, perhaps most notably between functional magnetic resonance imaging (fMRI) and electroencephalography (EEG). For example, fMRI studies typically use full field stimulus presentations and report bilateral IPS activation, whereas EEG studies direct attention to a single hemifield and report a contralateral bias in both hemispheres. Here, we addressed this question by applying a regions-of-interest fMRI approach to elucidate IPS contributions to WM. Importantly, we manipulated stimulus type (verbal, visuospatial) and the cued hemifield to assess the degree to which IPS activations reflect stimulus specific or stimulus general processing consistent with the pure storage or internal attention hypotheses. These data revealed significant contralateral bias along regions IPS0-5 *regardless* of stimulus type. Also present was a weaker stimulus-based bias apparent in stronger left lateralized activations for verbal stimuli and stronger right lateralized activations for visuospatial stimuli. However, there was no consistent stimulus-based lateralization of activity. Thus, despite the observation of stimulus-based modulation of spatial lateralization this pattern was bilateral. As such, although it is quantitatively underspecified, our results are overall more consistent with an internal attention view that the IPS plays a material general role in refreshing the contents of WM.

### 1. Introduction

The neural underpinnings of short-term or working memory (WM) remain a source of intense research interest. A host of converging evidence from various methodologies

© 2015 Published by Elsevier Ltd.

Address correspondence to: Marian E. Berryhill, PhD, University of Nevada, 1664 N. Virginia Street, Mail Stop 296, Reno, NV 89557, Tel: 775-682-8692, Fax: 775-784-1126, mberryhill@unr.edu.

**Publisher's Disclaimer:** This is a PDF file of an unedited manuscript that has been accepted for publication. As a service to our customers we are providing this early version of the manuscript. The manuscript will undergo copyediting, typesetting, and review of the resulting proof before it is published in its final citable form. Please note that during the production process errors may be discovered which could affect the content, and all legal disclaimers that apply to the journal pertain.

implicates the intraparietal sulcus (IPS) in WM (fMRI: Cowan, 2011; Majerus et al., 2007; Majerus et al., 2014; Majerus et al., 2006; Song & Jiang, 2006; Todd & Marois, 2004; Xu & Chun, 2006; but see: Mitchell & Cusack, 2007; EEG: Klaver, Talsma, Wijers, Heinze, & Mulder, 1999; Vogel & Machizawa, 2004; MEG: Mitchell & Cusack, 2011; Palva, Monto, Kulashekhar, & Palva, 2010; neurostimulation: Herwig et al., 2003; and neuropsychology, reviewed in: Berryhill, 2012; Olson & Berryhill, 2009). However, although there is general agreement supporting IPS involvement in some aspect of WM, the nature of these contributions remains unclear. It is important to clarify this question to adjudicate between different theoretical accounts.

Perhaps the best known account reflects the Multicomponent Model's view that short-term memory for verbal information requires the phonological loop, whereas visuospatial information relies on the visuospatial sketchpad for maintenance of visuospatial information and any multimodal maintenance depends on the episodic buffer (Baddeley, 1986, 2000; Baddeley & Hitch, 1974; Repovs & Baddeley, 2006). These components have been attributed to cortical locations based largely on patient work and functional neuroimaging data such that the left supramarginal gyrus is linked with the phonological loop, the right parietal lobe as a putative location for the visuospatial sketchpad, and the angular gyrus as the episodic buffer (Baddeley, 2003; Chein, Ravizza, & Fiez, 2003; Vilberg & Rugg, 2008). This view, that the IPS is engaged in a material specific role in WM, can be considered a *pure storage* account. Lateralized IPS activity would reflect the nature of the contents of WM, with unilateral left IPS activity for verbal stimuli and unilateral right IPS activity for visuospatial stimuli, rather than the spatial location at encoding of the to-be-remembered stimuli. Under the pure storage account, bilateral activations would not be expected for stimulus specific WM tasks and a contralateral bias would be dependent on the nature of the stimuli in use rather than their spatial location.

A competing perspective suggests that IPS activity represents a domain general process reflecting the storage and attentional refreshing of items in WM (Berryhill, Chein, & Olson, 2011; Chein & Fiez, 2010; Chein et al., 2003; Kiyonaga & Egner, 2013; Lewandowsky, Oberauer, & Brown, 2009; Majerus et al., 2014). In essence, the IPS is thought to keep elements in WM active by returning them to the focus of attention. The *internal attention* view predicts that bilateral IPS involvement reflects the attentional refreshing of items held in WM, regardless of the task demands (e.g., verbal or visuospatial). This attentional role could be covert and coincident with more explicit rehearsal strategies that are stimulus specific, such as subvocal rehearsal of verbal stimuli. Importantly, therefore, it does not prohibit the emergence of a stimulus-dependent hemispheric asymmetry due to the usage of additional rehearsal strategies. This interpretation is consistent with attentional models of WM (e.g., Barrouillet & Camos, 2009; Cowan, 1999; Unsworth & Engle, 2007).

Although these predictions regarding the IPS may seem straightforward, we quickly encounter a thicket of seemingly inconsistent findings from different research fields. Within each experimental approach there is general agreement regarding the nature of IPS activity during WM, but disagreement across experimental approaches. For example, the fMRI literature reliably identifies *bilateral* IPS activity reflecting the number of items currently maintained in WM (Song & Jiang, 2006; Todd & Marois, 2004; Xu, 2007; Xu & Chun,

2006; for a recent meta-analysis see: Rottschy et al., 2012). Importantly, the amplitude of these activations increases until it asymptotes at an individual's WM capacity limit (Todd & Marois, 2005). It is worth noting that these types of fMRI investigations use centrally placed visual stimulus arrays and identify bilateral activations along the lateral IPS.

In contrast, the EEG literature focuses on a slow component from posterior electrode sites that emerges during WM maintenance (Gao et al., 2009; Ikkai, McCollough, & Vogel, 2010; Jolicoeur, Brisson, & Robitaille, 2008; Klaver et al., 1999; McCollough, Machizawa, & Vogel, 2007; Vogel & Machizawa, 2004; reviewed in Drew, McCollough, & Vogel, 2006). It is known by two names: the sustained posterior contralateral negativity (SPCN) and the contralateral delay activity (CDA, the term used throughout this manuscript). In these studies, participants maintain central fixation and are cued to covertly attend to visual stimuli presented in either the left or right hemifield. Here, the CDA is derived from electrodes positioned over posterior parietal sites and a pattern emerges during WM maintenance showing greater activity for stimuli presented contralaterally compared to stimuli presented ipsilaterally. Again, the increase in amplitude corresponds to an individual's behavioral WM capacity limit (Anderson, Vogel, & Awh, 2011; Vogel, McCollough, & Machizawa, 2005). The source of this slow component is thought to be in the IPS (Mitchell & Cusack, 2011).

These conflicting findings might appear to be a simple issue of differing conventions across techniques. A few studies have focused on resolving discrepancies between the data from different methodologies (Bray, Almas, Arnold, Iaria, & MacQueen, 2015; Cutini et al., 2011; Robitaille et al., 2010; Sheremata, Bettencourt, & Somers, 2010), but they have reached different conclusions. For example, Sheremata and colleagues cued covert attention to oriented bars in one or both visual fields. They reported a contralateral bias in the left IPS, particularly in posterior portions, but no such contralateral bias in the right IPS. However, using a different spatial WM task Bray et al. (2015) compared IPS activity as a function of hemifield and observed a general contralateral bias for WM maintenance that became bilateral when maintenance demands required manipulation (Bray et al., 2015). In contrast, Robitaille and colleagues recorded fMRI, MEG and EEG data in the same participants while they performed a visuospatial WM task in a cued visual hemifield. Unexpectedly, they found bilateral IPS activity when looking at the fMRI data, but different components of the MEG data revealed both contralaterally driven and bilateral signals from posterior sites. They concluded that fMRI and EEG/MEG signals reflect different underlying neural processes. Cutini and colleagues reached a similar conclusion using a functional near-infrared spectroscopy (fNIRS) approach. They observed bilateral activations at detectors above the IPS even when unilateral encoding cues were provided. In summary, even when researchers have tried to assimilate the fMRI and EEG findings they have not achieved a consistent explanation.

An additional relevant consideration arises from the vision and attention literatures regarding what is represented in IPS regions. Visual attention relies on balanced activity in bilateral IPS regions; when one hemisphere is damaged this balance is disrupted and attentional deficits such as neglect or extinction emerge (e.g., Kinsbourne, 1977). The fact that hemispatial neglect more often follows right hemisphere lesions has led to the

hemispatial attention hypothesis, under which the right hemisphere controls attention to the full visual field whereas the left hemisphere controls attention to the right visual field alone (Heilman & Van Den Abell, 1980; Mesulam, 1981). However, fMRI studies have revealed that both the left and right IPS contain a set of topographic regions (IPS0-5) defined by their contralateral attentional or perceptual bias (Konen & Kastner, 2008; Schluppeck, Glimcher, & Heeger, 2005; Sereno, Pitzalis, & Martinez, 2001; Silver, Ress, & Heeger, 2005; Swisher, Halko, Merabet, McMains, & Somers, 2007); reviewed in: (Silver & Kastner, 2009). In other words, for visual attention tasks various IPS regions show a clear contralateral bias and this bias permits the mapping of IPS regions of interest. Furthermore, disrupting the IPS using transcranial magnetic stimulation (TMS) predictably shifts the corresponding behavioral bias farther toward the ipsilateral side (Battelli, Alvarez, Carlson, & Pascual-Leone, 2009; Brighina et al., 2002; Fierro et al., 2000; Plow et al., 2014; Pourtois, Vandermeeren, Olivier, & de Gelder, 2001; Szczepanski & Kastner, 2013). Thus, to address the mechanism of IPS in WM using fMRI it seems essential to cue the relevant visual hemifield (Sheremata et al., 2010) lest the WM responses be confounded by the bottom-up representation.

Incorporating the attended hemifield into consideration produces different predictions from the pure storage and internal attention classes of models. An internal attention model of WM can account for a contralateral bias in the IPS because it is stimulus general. The presence of contralateral bias is not strongly a function of the type of stimuli (verbal or visuospatial) to be remembered but rather a function of where the attended stimuli were located during encoding. A contralateral bias would pose a greater challenge for the pure storage view. This is because the pure storage model hypothesizes a material specific hemispheric lateralization revealing left IPS activity for verbal stimuli and right IPS activity for visuospatial stimuli. Thus, a unilateral contralateral bias would strongly depend on the stimulus category. The consequence for behavior would be that the pure storage account would predict significantly worse verbal WM performance for stimuli presented on the left and worse visuospatial WM performance for stimuli on the right.

To adjudicate between the pure storage and internal attention accounts, we investigated whether IPS activity during WM reflects a stimulus specific or a stimulus general process. A stimulus specific process consistent with the pure storage view predicts hemispheric lateralization solely as a function of stimulus type (left: verbal; right: visuospatial), regardless of where the stimulus is located on the display (left or right hemifield). In contrast, a stimulus general mechanism consistent with the internal attention view predicts bilateral activation regardless of stimulus type and location. To summarize, contralateral IPS activation after cueing attention to a single visual field would support the internal attention hypothesis. In contrast, a consistent left IPS/language, right IPS/visuospatial representation regardless of encoding hemifield would provide strong evidence for the pure storage account.

## 2. Methods

### 2.1 Participants

Ten observers (two females, 23-45 years of age) participated in the experiment. All observers, with the exception of one, were right-handed, all reported normal or corrected-to-normal vision, and all were in good health with no history of neurological disorders. Each observer gave written informed consent prior to participating in the experiment according to the guidelines of the University of Nevada Reno Internal Review Board and the University of California Davis Imaging Research Center. All participants, except one, were run in three scanning sessions: one for high-resolution anatomical images, one for retinotopic mapping, and one for the main experiment. One participant was not run in the retinotopic mapping scans due to a scanner malfunction. We note that for all analyses the same pattern of data were observed when all participants were included, and when we excluded either or both the left-handed participant or the participant for whom we used an atlas to define IPS ROIs.

### 2.2 Apparatus and Display

The stimulus computer was a 2.53 GHz MacBook Pro with an NVIDIA GeForce 330M graphics processor (512MB of DDR3 VRAM). Stimuli were generated and presented using the Psychophysics Toolbox (Brainard, 1997) for MATLAB (Mathworks Inc., Natick, MA). Stimuli were presented on a Cambridge Research System (Kent, UK) LCD BOLDscreen display (60-Hz refresh rate) outside of the scanner bore and viewed by way of a tangent mirror attached to the head coil, which permitted a maximum of visual area of  $19.3^\circ \times 12.1^\circ$ . Across experiments, stimulus presentation was time-locked to functional MRI (fMRI) acquisition via a trigger from the scanner at the start of image acquisition.

### 2.3 MRI Apparatus/Scanning Procedures

All data were acquired at the University of California Davis Imaging Research Center on a 3T Skyra MRI System (Siemens Healthcare, Erlangen, Germany) using a 64 channel phased-array head coil. Functional images were obtained using T2\* fast field echo, echo planar functional images (EPIs) sensitive to BOLD contrast (WM task: TR = 2 s, TE = 25 ms, 32 axial slices, 3.0 mm<sup>2</sup>, matrix size = 80 × 80, 3.5 mm thickness, interleaved slice acquisition, 0.5 mm gap, FOV = 240 × 240, flip angle = 71°; retinotopic mapping: same, except 32 axial slices, TR = 2.5 s). High-resolution structural scans (MPRAGE: 208 sagittal slices, 0.9 mm<sup>2</sup> in-plane voxel resolution, matrix size = 256 × 256, slice-thickness = 0.95 mm, FOV = 243 × 243 × 187 mm, TE = 4.33 ms, TR = 10 ms, flip angle = 7°) were collected to support reconstruction of the cortical hemisphere surfaces using FreeSurfer (<http://surfer.nmr.mgh.harvard.edu> Dale, Fischl, & Sereno, 1999; Fischl, Sereno, & Dale, 1999).

### 2.4 Retinotopic Mapping

We defined a series of topographic regions of interest (ROIs) on each participant's cortical surfaces using AFNI (<http://afni.nimh.nih.gov/afni/> Cox, 1996), SUMA (<http://afni.nimh.nih.gov/afni/suma>, (Saad, Reynolds, Cox, Argall, & Japee, 2004). Standard retinotopic mapping was performed for each participant using a color and luminance varying

flickering (4 Hz) checkerboard stimulus (Arcaro, McMains, Singer, & Kastner, 2009; Swisher et al., 2007). Participants performed 8 runs (3 runs for one participant) of polar angle mapping and 2 runs (1 run for one participant) of eccentricity mapping.

For half of the polar angle mapping runs, the moving wedge covered a 45° angle and spanned from 0.5° to 13.5° eccentricity; for the other half, the wedge spanned from 8° to 13.5° eccentricity. The later trials were included to limit stimulation of the central portion of visual space since voxels in higher-order topographic regions may be stimulated by all wedge positions, decreasing the spatial specificity of the signal during polar angle mapping (Dumoulin & Wandell, 2008). Polar angle mapping runs comprised of eight 40-s stimulus cycles (speed of 9°/s) with a 20-s blank period at the beginning of each run. Consecutive runs alternated between a clockwise and counterclockwise wedge rotation.

For the eccentricity mapping runs, the stimulus was a moving ring with a 1.7° width along eccentricity. Over a single cycle, the ring traversed the space between 0° and 13.5° eccentricity from fixation. All eccentricity mapping runs were comprised of eight 40-s stimulus cycles (speed of 9°/s) with a 10-s blank period interleaved between cycles and a 20-s blank period at the beginning of each run. The addition of a blank period between cycles avoids the potential ambiguity in discerning central fovea and far periphery representations when the ring stimulus immediately wraps around upon reaching the near or far extreme of the stimulus extent. Consecutive runs alternated between expanding and contracting ring movements.

For both polar angle and eccentricity mapping, participants were instructed to maintain fixation on a central spot while covertly attending to the wedge or ring stimulus and to report via a button press the onset of a uniform gray patch in the stimulus that served as the target. Targets appeared, on average, every 4.5 s.

Polar angle and eccentricity representations were extracted using standard phase encoding techniques (Bandettini, Jesmanowicz, Wong, & Hyde, 1993; Engel, Glover, & Wandell, 1997; Sereno et al., 1995). Borders between adjacent topographic areas of the IPS were defined by reversals in polar angle representations at the vertical meridians. Six topographically organized areas were identified in the posterior parietal cortex (Konen & Kastner, 2008; Schluppeck et al., 2005; Sereno et al., 2001; Silver et al., 2005; Swisher et al., 2007). Each area contained a representation of the contralateral visual field and was separated from neighboring areas by reversals in the progression of polar angle representation. Anterior to IPS0 (i.e., V7), IPS1 and IPS2 were located in the posterior part of the IPS, IPS3 and IPS4 were located in the anterior-lateral branch of the IPS, and IPS5 extended into the intersection between the IPS and the postcentral sulcus. See Figure 4 for ROIs delineation in a representative participant.

For the one participant for which individual retinotopic mapping scans could not be collected we utilized a probabilistic atlas of visual topography in human cortex derived from a large number of participants (Wang, Mruczek, Arcaro, & Kastner, 2014). Briefly, the probabilistic atlas contains a “maximum probability map” indicating the most probable ROI label for each coordinate within a standard surface-based space (Fischl, Sereno, Tootell, &

Dale, 1999). For the participant from the current study, the individual's reconstructed cortical surface was warped to the same standard surface space, and then the maximum probability map was used to label surface nodes in the IPS as IPS0-5. Subsequently, these atlas-derived ROIs were projected back to the participant's native cortical space and subsequently treated in the same manner as the individually mapped ROIs for all other participants.

For the purpose of reporting standard coordinates of IPS0-5, we transformed each subject's anatomic volume into Talairach space (Talairach & Tournoux, 1988) using AFNI's @auto\_tlrc function. The resulting transformation matrix was then used to convert the center-of-mass coordinates, determined from the cortical surface projection of each ROI, into Talairach space (Table 1).

## 2.5 Visual Working Memory Task

The participants performed a change detection WM task. During each trial, sixteen items appeared on the screen, eight in each hemifield. Three items were designated as targets by their color (targets were red, distractors were blue). After a brief delay (fixation spot remained visible), the stimulus array reappeared. On 50% of the trials, a feature value of one target item changed. Participants indicated whether or not there was a change by making a button press response (left index finger for 'no change', right index finger for 'change'). Each trial lasted 6 s (100 ms sample array, 900 ms delay period, 2 s test array, and 3 s inter-trial interval). Participants were asked to fixate a central black and white square ( $0.25^\circ$ ) throughout the experiment.

The different conditions of the experiment were defined based on stimulus type (oriented bars, letters), the visual field location of the to-be-remembered targets (left, right, or either hemifield), and the specific task (WM, passive viewing) for each trial. Stimuli were bars ( $0.9^\circ \times 0.33^\circ$ ) with a horizontal or vertical orientation, or were the letters 'R' or 'K' ( $1.2^\circ \times 0.5^\circ$ ). In the stimulus array, targets were randomly assigned one of the two possible feature values, with the constraint that all targets could not have the same value. In terms of visual field location, cues indicated that the targets would appear in the left, right, or either hemifield. Note that in the either hemifield condition targets were confined to a single hemifield, but the specific hemifield was unpredictable within a trial block (see below). Additionally, stimuli were always presented to both the left and right hemifields (i.e., full-field presentation), but participants only performed the WM task in one hemifield on each trial (defined by target location). In terms of the task manipulation, the WM trials proceeded as described above. In contrast, for the passive viewing task, participants were not required to remember anything about the sample array targets. Rather, they simply responded with a button press as soon as the test array appeared. Thus, participants attended to the stimuli during passive viewing trials, but were not required to remember the stimulus array.

Individual trials were presented in blocks of 6 continuous trials, with each of the trials in a block belonging to the same condition (i.e., same stimulus type, hemifield location, and task). Prior to the start of each block, a cue indicated which conditions (stimulus type, hemifield location, and task) the upcoming block would contain; see Figure 1. The cues were solid circles offset  $2^\circ$  from central fixation with a radius of  $0.5^\circ$ . The location of the

cue (left, right, or both) indicated the side that the target stimuli would appear (left, right, or either), and thus the hemifield location of the memory task. A circle surrounding the fixation square indicated that the upcoming block required passive viewing. For all blocks, the cue color (black or white) indicated which stimulus type (oriented bars or letters) would be presented during that block. The cue was displayed for 2 s, which was followed by an additional 2 s blank period before the onset of the first trial in the block.

Each run included eight 40 s blocks (4 s cue period plus six 6 s trials) with a 16 s blank period at the start and end of each run. Each run contained one block of each of the following conditions: six WM blocks (2 stimulus types  $\times$  3 hemifield locations) and 2 passive viewing blocks (one for each stimulus types, with a randomly selected hemifield location). Participants completed 7 runs, each lasting 5 min and 52 s, for a total scan time of 46 min 56 s.

After each fMRI session, we included an explicit strategy check that the stimuli were perceived verbally (letter stimuli) and visuospatially (oriented bar stimuli). In a written questionnaire, participants reported the strategies they used in remembering the different stimulus types and whether they found one task more difficult than another. The majority of participants (9/10) reported that when the stimuli were letters they would subvocally repeat the letters until the probe phase, and remember the stimulus order from top to bottom. For the oriented bars, half of the participants (5/10) reported perceptually grouping the bars into a more global pattern to remember them. For example, one participant reported that they would remember the bars as a shape or spatial pattern. No participants reported using a nonverbal strategy for the letters or a verbal strategy for the oriented bars, or any other strategy.

## 2.6 Behavioral Data Analysis

Visual short-term WM was assessed using Cowan's K (Cowan, 2001), defined as

$$K = SS \times (HR - FA)$$

where SS represents the set size (always 3 target items in the current experiment), HR the hit rate, and FA the false alarm rate. The hit rate represents the proportion of correct responses for trials in which there was a change in one of the target's feature values. The false alarm rate represents the proportion of incorrect responses for trials in which there was no change. The K score represents the number of objects a participant holds in WM. The K score was calculated for each run and participant, separately for each hemifield location and stimulus type.

## 2.7 fMRI Preprocessing and Data Analysis

Functional fMRI data were analyzed using AFNI (<http://afni.nimh.nih.gov/afni/Cox>, 1996), SUMA (<http://afni.nimh.nih.gov/afni/suma>, (Saad et al., 2004), FreeSurfer (<http://surfer.nmr.mgh.harvard.edu> Dale et al., 1999; Fischl, Sereno, & Dale, 1999), MATLAB, and SPSS Statistics 19 (IBM, Armonk, NY). Functional scans were slice-time corrected to



the first slice of every volume and motion corrected within and between runs. The anatomical volume used for surface reconstruction was aligned with the motion-corrected functional volumes and the resulting transformation matrix was used to provide alignment of surface-based topographic ROIs with the volume-based WM dataset.

Functional images were smoothed with a 6-mm Gaussian kernel and normalized to percent signal change by dividing the voxel-wise time series by its mean intensity in each run. The response during each condition (i.e., stimulus type  $\times$  attended hemifield location  $\times$  task) was quantified in the framework of the general linear model (Friston, Frith, Turner, & Frackowiak, 1995). Square-wave regressors for each unique block type and cue were generated and convolved with a response model (BLOCK model in AFNI's 3dDeconvolve function) accounting for the shape and temporal delay of the hemodynamic response. Nuisance regressors were included to account for variance due to baseline drifts across runs, linear and quadratic drifts within each run, and the six-parameter rigid-body head motion estimates.

For the group-level whole-brain analysis each individual's reconstructed cortical surface was warped to a standard surface-based space (Fischl, Sereno, Tootell, et al., 1999) and then resampled in SUMA using an icosahedral shape to generate a standard mesh with a constant number of co-registered nodes (Argall, Saad, & Beauchamp, 2006). Statistical maps were calculated using a mixed-effects meta-analysis that accounted for both within- and between-participant variance (AFNI's 3dMEMA, <http://afni.nimh.nih.gov/sscc/gangc/MEMA.html>).

Unsmoothed data were used for analyses based on individually defined ROIs (IPS0-5). Additionally, these data were not spatially normalized and remained the in each participant's native space. The average time series was extracted from unsmoothed data after linear trend removal. In each ROI, voxel selection was restricted to the 50 voxels with the most significant activation from any of the WM conditions, compared to baseline. Because of limited ROI size, the 50-voxel criteria could not be met for 5 (out of 120) possible participant-hemisphere-ROIs, in which case all of the voxels from that ROI were included in the analysis (minimum of 31 voxels). The mean response to each condition was calculated as the average evoked response across a 38 s (19 TRs) window starting at 2 s after block onset. To directly compare the mean response across selected conditions we calculated a  $d'$  index (Afrac, Kiani, & Esteky, 2006; Mruczek, von Loga, & Kastner, 2013; Pinsk, DeSimone, Moore, Gross, & Kastner, 2005):

$$d' \text{ index} = (\mu_{\text{cond1}} - \mu_{\text{cond2}}) / \sqrt{[(\sigma^2_{\text{cond1}} + \sigma^2_{\text{cond2}}) / 2]}$$

where  $\mu$  and  $\sigma^2$  are the blockwise mean and variance, respectively, of the evoked response for a given condition. The  $d'$  index scales the difference across two conditions (cond1 and cond2) by a measure of the overall variance and is positive when cond1 > cond2 and negative when cond1 < cond2, with larger values indicating greater separation.

Differences in mean BOLD activation and  $d'$  indices were compared using a repeated-measures ANOVA. For all ANOVAs violations of sphericity, as indicated by Mauchly's test, were corrected using the Greenhouse-Geisser correction.

### 3 Results

#### 3.1 Visual Working Memory: Behavioral Performance

We first investigated participants' performance as a function of stimulus type and attended hemifield location using Cowan's K, an estimate of WM capacity. Participants' K scores were fairly consistent across conditions (letters: left hemifield,  $M = 1.91$ ,  $SD = 0.12$ ; right hemifield,  $M = 2.14$ ,  $SD = 0.11$ ; either hemifield,  $M = 1.75$ ,  $SD = 0.17$ ; oriented bars: left hemifield  $M = 2.07$ ,  $SD = 0.12$ ; right hemifield,  $M = 1.93$ ,  $SD = 0.23$ ; either hemifield,  $M = 2.12$ ,  $SD = 0.16$ ); see Figure 2. A  $2 \times 2$  ANOVA (stimulus type  $\times$  hemifield location) limited to the left and right hemifield trials revealed no significant main effects (stimulus type:  $F_{(1,9)} = 0.08$ ,  $p = .78$ ; hemifield location:  $F_{(1,9)} = 0.21$ ,  $p = .66$ ) or interactions ( $F_{(1,9)} = 1.91$ ,  $p = .20$ ). Although not significant, there was a numerical trend toward lower K scores for letter targets in the left hemifield and lower K scores for the oriented bar target in the right hemifield. This ANOVA was restricted to these conditions because our predictions were restricted to these conditions rather than the either hemifield condition, which collapsed across presentation hemifield.

#### 3.2 Whole-Brain Analyses

First, to confirm IPS involvement in WM we performed a whole-brain analysis comparing WM activation to passive viewing. We contrasted each of the WM conditions (2 stimulus types  $\times$  3 hemifield locations) with the passive viewing condition separately and identified voxels with significantly more activity during any of the WM conditions than during passive viewing (Figure 3A). Thus, this analysis makes *no assumptions* about the laterality of activation or task related activity. In general, there were broad IPS activations during the WM task. Thus, the whole-brain group analysis confirmed WM-related activity is evident in the IPS ROIs examined more closely below. Second, to investigate general patterns of contralateral bias, collapsing across stimulus type, we contrasted hemifield of presentation (right  $>$  left; see Figure 3B). Here, we saw a general pattern of contralateral bias with a concentration along the IPS. Additionally, if anything, the contralateral bias was stronger in the right hemisphere. Finally, to investigate the presence of stimulus-based differences we contrasted the two stimulus types (verbal (letters)  $>$  visuospatial (oriented bars); Figure 3C). This analysis shows that although some stimulus-based differences emerge along the IPS, they were not lateralized to one hemisphere. In summary, these whole-brain analyses applied relatively liberal thresholds to confirm that we did not miss large clusters of activity that would speak to our questions of interest. Importantly, it confirms that the ROIs along the IPS activate during WM in general, but with nuances reflecting stimulus location (right vs. left hemifield) and stimulus type (letters vs. oriented bars). To address these more focused questions more powerful ROI-based analyses follow.

### 3.3 Region of Interest Analyses

To explore the differences in activation across stimulus type, hemifield, and IPS ROI, we proceeded with a ROI-based timecourse analysis. Timecourses of BOLD activation were extracted from each ROI (IPS0-5, Figure 4), in each hemisphere independently, starting 6 s prior to the start of the first trial in each block and ending at 40 s after the start of the block; see Figure 5. This time window encompassed the cue period and the six 6-s trials of each block. We compared the mean BOLD signal change across conditions using a  $d'$  index (see Methods). First, we focus on WM-related activity (either hemifield vs. passive viewing). In the subsequent section, we discuss the laterality of activation by stimulus location (left vs. right hemifield) and stimulus type (letters vs. oriented bars). Importantly, ROI analyses in topographically mapped IPS regions were consistent with previous relevant findings identifying functional (Sheremata et al., 2010; Trapp & Lepsien, 2012) or structural and functional connectivity (Bray, Arnold, Iaria, & MacQueen, 2013) differences between posterior and anterior IPS regions. This analysis addressed modulation in response along the IPS as a function of task, contralateral bias, and stimulus type.

**3.3.1 WM-related Activity**—Consistent with the whole-brain analysis, the ROI analysis confirmed greater activation during the WM task (either hemifield condition) compared to the passive viewing task; see Figure 5A, B. We compared the mean BOLD signal across the block of six consecutive trials from the WM (either hemifield) and passive viewing conditions, separately for each ROI, hemisphere, and stimulus type using a 4-way ANOVA (ROI  $\times$  hemisphere  $\times$  stimulus type  $\times$  task). Directly related to the competing predictions of the internal attention and pure storage models, this analysis revealed a main effect of task ( $F_{(1,9)} = 6.07, p = .036$ ). The WM task led to significantly greater activation than the passive viewing task in every ROI, in both hemispheres, and for both stimulus types. There was also a significant three-way interaction between hemisphere, ROI, and task ( $F_{(5,45)} = 3.17, p = .016$ ), driven by the greater difference between the WM and passive viewing tasks for right hemisphere IPS2 and IPS3 ROIs. Finally, there was a marginally significant interaction between ROI  $\times$  stimulus type ( $F_{(2,09,18,8)} = 2.86, p = .08$ ), which reflects the fact that the letter stimuli led to stronger activations for all but the most anterior IPS regions (IPS4/5). No other main effects or interactions approached significance (all  $p$ 's  $> .11$ ).

To further explore WM-related activity in topographic regions of the IPS, we evaluated the  $d'$  index to more directly compare the difference in activation across the WM and passive viewing tasks. In this case, the  $d'$  index represents the normalized difference in mean activity between the WM and passive viewing conditions, with positive values indicating stronger activation for the WM task. A 3-way ANOVA (ROI  $\times$  hemisphere  $\times$  stimulus type) revealed no significant main effects or interactions; see Figure 5C. There was a marginal main effect of ROI ( $F_{(2,7,24,2)} = 2.40, p = .098$ ) due to WM-related activity in IPS0 being lower than in more anterior regions. This is also apparent in the group-level analysis described above and in the timecourse analysis just described. But overall, this analysis confirmed that WM-related activity was observed throughout the IPS, in both hemispheres, regardless of the stimuli used. No other main effects or interactions reached significance (all  $p$ 's  $> .11$ ).

This analysis, which included the either hemifield WM condition, allowed us to examine the differences between passive viewing and working memory without having contamination from pre-trial attentional allocation. Because the stimulus could be presented in either hemifield, this ensured that participants could not pre-allocate attention before the trial started.

In summary, we found that activation of topographic regions of the IPS was greater during the WM task than the passive viewing task, that this difference was consistent across both hemispheres and across both stimulus types. The only statistical trend was for weaker WM-related activation in posterior IPS areas (IPS0) compared to more anterior areas (IPS1-5).

**3.3.2 Contralateral Bias**—To explore the presence of any contralateral bias in the IPS during WM, we compared the evoked BOLD response across blocks in which participants attended to stimuli presented in the left or right visual field (hemifield location) while performing either the verbal or visuospatial WM task (stimulus type). It is worth reiterating that visual stimuli were presented to both hemifields in all trials. Consequently, any observed differences are due to WM task demands rather than low-level visual stimulation.

We compared the mean BOLD signal across the block of six consecutive trials from the two attended hemifield locations (left, right), for each ROI, hemisphere, and stimulus type using a 4-way ANOVA (ROI  $\times$  hemisphere  $\times$  stimulus type  $\times$  hemifield location); see Figure 6. This analysis did not reveal any significant main effects (all  $p$ 's  $> .15$ ). Importantly, the presence of a contralateral bias was established by the presence of a significant interaction between hemisphere and hemifield location ( $F_{(1,9)} = 59.2, p < .001$ ). During the WM task, there was greater right hemisphere activation after attending to stimuli in the left hemifield, and greater left hemisphere activation after attending to stimuli in the right hemifield. Furthermore, there was a significant 3-way interaction between hemisphere, hemifield location, and ROI ( $F_{(5,45)} = 3.18, p = .015$ ). This interaction reflects a weaker contralateral bias in more anterior regions (IPS2-5) compared to posterior regions (IPS0-1), particularly in left hemisphere ROIs.

Finally, it is relevant to note the marginally significant interaction between hemifield location and stimulus type ( $F_{(1,9)} = 4.80, p = .056$ ). Here, there was a trend for the letter stimuli to lead to stronger activations when presented in the right hemifield, and for the orientation task to lead to stronger activations when presented in the left hemifield.

To further explore what factors influence the contralateral bias in topographic regions of the IPS observed during the WM task, we calculated a  $d'$  index to more directly compare the difference in activation across the two possible hemifield locations. For this analysis, we recoded left and right hemifield locations as contralateral and ipsilateral with respect to each cortical hemisphere. Thus, the  $d'$  index represents the difference between the mean activation when the WM task was performed in the contralateral vs. ipsilateral hemifield, with positive values indicating stronger activation for the contralateral condition (i.e., stronger contralateral bias). A 3-way ANOVA (ROI  $\times$  hemisphere  $\times$  stimulus type) revealed a significant main effect of ROI ( $F_{(5,45)} = 13.1, p < .001$ ); see Figure 6C. Contralateral biases were greater in more posterior IPS areas (IPS0-1) than in more anterior ones (IPS2-5).

We also observed a significant hemisphere  $\times$  stimulus type interaction ( $F_{(1,9)} = 6.11, p = .036$ ), driven by stronger contralateral bias for the letter stimuli in the left hemisphere and stronger contralateral bias for the oriented bar stimuli in the right hemisphere. No other main effects or interactions approached significance (all  $p$ 's  $> .29$ ).

**3.3.3 Contrast of Letters and Oriented Bar Stimuli**—The contralateral bias analysis revealed some hemispheric differences depending on the stimulus type (letters vs. oriented bars). However, it remained unclear whether these differences reflect a significantly *lateralized* recruitment of the IPS dependent on stimulus type, as predicted by the pure storage model of WM, or if they reflect a stimulus type-dependent modulation of an underlying spatial bias, as allowed by the internal attention model of WM. To address this question, we calculated a  $d'$  index to directly compare the difference in activation across the two stimulus types, as a function of hemisphere, and visual hemifield of the remembered targets. For this analysis, the  $d'$  index represents the normalized difference in mean activity between the letter and oriented bar stimuli, with positive values indicating stronger activation for the verbal stimuli (letters) and negative values indicating stronger activation for the visuospatial stimuli (oriented bars). Accordingly, pure storage predicts a main effect of hemisphere reflecting all positive  $d'$  index values in the left hemisphere (reflecting recruitment for verbal stimuli) and all negative  $d'$  index values in the right hemisphere (reflecting recruitment for visuospatial stimuli). In contrast, internal attention predicts no significant  $d'$  value differences across hemispheres and stimulus types, consistent with little stimulus-based bias.

A 3-way ANOVA (ROI  $\times$  hemisphere  $\times$  hemifield location) revealed a significant main effect of hemifield ( $F_{(1,9)} = 6.09, p = .036$ ); see Figure 7. Across both hemispheres and all IPS ROIs, the oriented bar stimuli led to stronger activation when the task was performed in the left visual hemifield (light gray bars), whereas the letter stimuli led to stronger activation when the task was performed in the right visual hemifield (dark gray bars). Additionally, we observed a marginally significant three-way ROI  $\times$  hemisphere  $\times$  hemifield location interaction ( $F_{(5,45)} = 2.32, p = .059$ ), although it is not obvious what drives this trend. Importantly, these results are not consistent with the pure storage model because there was no significant main effect of hemisphere ( $F_{(1,9)} = 0.68, p = .43$ ). No other main effects or interactions approached significance (all  $p$ 's  $> .34$ ).

In summary, we observed a contralateral bias in each IPS ROI. This contralateral bias was stronger in the right hemisphere for the oriented bar stimuli and a stronger in the left hemisphere for the letter stimuli. However, we did not observe any hemispheric lateralization activity based on stimulus type. Letter stimuli led to stronger IPS activation when presented in the right hemifield, and oriented bar stimuli led to stronger IPS activation when presented in the left hemifield, but this was consistently observed for both the left and right hemispheres.

## 4. Discussion

Here, we probed the nature of the neural correlates of WM in the IPS. In particular, we evaluated the presence or absence of a contralateral bias in IPS ROIs and investigated

whether there was stimulus specific or stimulus general activation patterns. To summarize our findings, first we confirmed bilateral IPS involvement in WM tasks by showing significantly stronger activations elicited by the WM task than the passive viewing control task. Importantly, this pattern was present across all of the topographic regions of interest (IPS0-5). Second, we observed consistently stronger activations when the WM task was performed in the contralateral hemifield across all IPS ROIs and for both stimulus types. Notably, this contralateral bias was stronger in the left hemisphere for the letter stimuli, and stronger in the right hemisphere for the oriented bar stimuli. Importantly, there was a similar stimulus-based bias in *both* hemispheres such that IPS responses were greater for the oriented bar stimuli when the memory targets were in the left hemifield and letter stimuli when the memory targets were in the right hemifield. The implications of these findings are discussed below.

#### 4.1 Theoretical Implications

One purpose of this study was to investigate the nature of IPS representations in WM. We tested competing predictions from the pure storage and internal attention classes of hypotheses regarding the role of the IPS in WM. Specifically, the *pure storage* model predicts left hemisphere involvement exclusively in verbal WM tasks and right hemisphere involvement exclusively in visuospatial WM tasks, regardless of the spatial location of the items at encoding. In contrast, the *internal attention* hypothesis predicts bilateral IPS engagement during WM tasks, regardless of the stimulus category, with a contralateral bias reflecting the spatial location of the remembered items.

Because the data showed that both the left and right IPS responded to verbal and visuospatial stimuli we interpret the present data as being more consistent with the internal attention hypothesis. As predicted by this model, the IPS responds strongly to stimuli held in WM and is thought to provide an attentional refresh of these items and protect them from decay. The representations themselves are likely elsewhere in the brain, for example in earlier sensory regions (e.g., Harrison & Tong, 2009; Serences, Ester, Vogel, & Awh, 2009). These data join other fMRI studies of WM revealing significant domain general processing in the IPS (Chein, Moore, & Conway, 2011; Cowan et al., 2011; Fedorenko, Duncan, & Kanwisher, 2013; Li, Christ, & Cowan, 2014). The current data add to these findings by showing that there is a contralateral bias in the representation of the items in WM related to the spatial location of the remembered items, but not a lateralization bias such that verbal information is exclusively maintained in the left IPS and visuospatial information in the right IPS, as predicted by the pure storage perspective. There is some nuance here, as well. We also observed *greater* contralateral bias in the left IPS for verbal stimuli and in the right IPS for visuospatial stimuli. This pattern of stimulus-based bias indicates some degree of hemispheric lateralization as a function of stimulus category. The internal attention hypothesis would offer that this extra bias reflects the addition of material-specific rehearsal mechanisms (e.g., phonological loop) to bolster WM performance. Thus, the internal attention model can accommodate *some* degree of stimulus-specific lateralization of function as long as each hemisphere reflects functional engagement during WM tasks. This flexibility could also be interpreted as a less stringent form of the internal attention model that includes an element of hemispheric laterality in a less categorical way than the pure

storage view. Unfortunately, the internal attention model is underspecified and it does not currently constrain the degree of stimulus-based bias that can be accommodated. This is a clear criticism of the internal attention view and future work is needed to quantify what degree of stimulus-based bias the model can tolerate. The pure storage model, on the other hand, has difficulty reconciling the observed space-based lateralization (i.e., contralateral bias) of the IPS with a lateralized stimulus-specific storage module. Thus, although there was a stimulus-based bias, it was similarly present in both hemispheres, contrary to the predictions of the pure storage view. In other words, although the predictions of the internal attention model were not perfectly met, these data remain more consistent with it because contralateral IPS activity was significant during the WM task regardless of stimulus type.

The calculation of contralateral activity might be sensitive to experimental factors such as the manner by which ROI's were mapped (see next section for more detailed discussion). However, this does not seem to be the case. Across different studies using a variety of approaches for defining ROIs, the IPS reflects bilateral activations during WM. For example, Xu and Chun (see also Todd & Marois, 2004; Xu & Chun, 2006) created inferior and superior IPS ROIs based on functional localizer tasks and found that visuospatial stimuli drove both the left and right inferior and superior IPS. Of relevance here are findings from Fiez and colleagues proposing functional dissociations between left dorsal and ventral IPS areas during verbal WM, with dorsal areas serving domain-general processes and ventral areas providing domain-specific phonological encoding processes (Becker, MacAndrew, & Fiez, 1999; Chein et al., 2003; Ravizza, Delgado, Chein, Becker, & Fiez, 2004). More recently, there is evidence for specialization within their ventral IPS region such that the left hemisphere is more involved in WM and perceptual processing whereas the right hemisphere is more involved in attention, and a bilateral anterior region is involved in WM retrieval (Langel, Hakun, Zhu, & Ravizza, 2014). The present data do not find support for this perspective, although the IPS ROIs we probed may not directly map on to their dorsal and ventral regions.

## 4.2 Comparison with Previous Studies

The current work is most similar to a recent fMRI paper exploring activation patterns in IPS ROIs during a visuospatial WM task (Sheremata et al., 2010). Sheremata and colleagues found a strong contralateral bias in the left IPS regions, especially IPS1-2, but no contralateral bias in the right IPS. This paper is particularly relevant to the current findings because the experimental designs were quite similar. To begin with the consistent findings across studies, we both observed greater IPS activity for WM-related activity than for passive viewing. We also both confirmed that this IPS activity was not due to the number of visual stimuli presented at encoding but rather due to WM-related engagement because the number of presented stimuli was equivalent in WM and passive viewing conditions. This addresses a limitation of some previous fMRI findings (e.g., (Todd & Marois, 2004; Xu & Chun, 2006). Both our study and the one by Sheremata and colleagues completed ROI analyses parceling IPS regions based on their topographic representations of visual space. We both report contralateral bias in the left IPS during WM. However, they did not observe a contralateral bias in the right IPS, whereas we observed a robust contralateral bias in the right IPS. Indeed, if anything, we observed a stronger contralateral bias in the right

hemisphere than in the left hemisphere. We also found robust WM responses throughout IPS0-5, whereas Sheremata et al. (2010) found their strongest WM responses exclusively in the most posterior IPS regions. However, Szczepanski et al. found greater contralateral bias in posterior left IPS in response to increased WM load compared to the response in posterior right IPS (Szczepanski, Konen, & Kastner, 2010). Very recently, Sheremata & Silver reported that the left, but not the right, hemisphere showed a greater contralateral bias in visual field representations (population receptive fields; pRFs) that were significantly enhanced by shifting attention from fixation to a peripheral stimulus (Sheremata & Silver, 2015). Of relevance here is a recent study that used multi-voxel pattern analysis and reported that attention increased the amplitude of responses, but not their spatial representation; but a pRF analysis did show attentional enhancement in the bilateral IPS0 ROI they probed (Sprague & Serences, 2013). Of considerable interest is a large study employing functional connectivity analyses that reports WM task demands modulate the contralateral bias in the IPS such that maintenance recruits IPS heavily contralaterally, whereas increased manipulation demands increase bilateral IPS contributions (Bray et al., 2015).

What might explain these discrepancies? One possibility is that there are subtle paradigmatic differences between these various experimental designs, the instructions or perhaps the populations tested. Most puzzling is the discrepancy with the report from Sheremata and colleagues (2010). They manipulated set size (1, 3, or 6 target) and used a single stimulus type (oriented bars). In contrast, we used a single set size (3 targets), for which they had seen the greatest effects, and included two stimulus types (oriented bars, letters). Overall, the Sheremata results are consistent with the neuropsychological literature showing hemifield neglect predominantly after lesions to the right parietal lobe (e.g., Heilman & Van Den Abell, 1980). Our current fMRI observations are more consistent with the existing EEG/CDA literature (e.g., Vogel & Machizawa, 2004), which relies on a bilateral contralateral bias from posterior parietal electrode sites. It is also consistent with fMRI findings reporting interhemispheric competition during attention tasks. For example, it is argued that the contralateral bias reflects the sum total of attentional weights throughout the IPS (e.g., Szczepanski & Kastner, 2013). The stimulus category may provide an additional weighting factor that enhances contralateral bias in a stimulus-specific way. For instance, by promoting greater contralateral bias for verbal stimuli in the right hemifield and reduced contralateral bias when verbal stimuli in the left hemifield. In addition, a shift in WM task demands from maintenance to manipulation will enhance the bilaterality of the IPS response (Bray et al., 2015). This raises the possibility that a participant's strategy in completing some tasks may also play a role in whether a strong or weak contralateral bias in the IPS is observed. A less satisfying possibility is that we face known concerns relating to the lack of reproducibility of fMRI research (Yarkoni, Poldrack, Van Essen, & Wager, 2010). Future replications and extensions will be needed to clarify the role of the IPS during WM.

### 4.3 Caveats and Future Directions

One possible concern is the fact that there were low-level features differences between the letter and oriented bars that may have influenced how participants perceived the stimuli or performed the tasks. However, behavioral differences between the verbal and visuospatial tasks were not significant, suggesting one task was not more difficult than another.



Furthermore, participants reported spontaneous use of verbal and visuospatial strategies for the two stimulus sets in post-experiment questionnaires. Finally, the finding of a modest bias in a canonical direction (left: verbal, right: visuospatial) suggests that these tasks drove the IPS in an expected direction.

Another concern is the lack of eye tracking to ensure that participants maintained central fixation. Yet, if participants were freely moving their eyes and fixating the stimulus arrays, any contralateral bias should be eradicated by stimulating both hemifields. In essence, if we had not observed a contralateral bias and failed to do eyetracking, it would be reasonable to argue that eye movements explained the data. Because our results show a contralateral bias regardless of stimulus type, it is less of a concern that participants did not maintain central fixation, as instructed.

Previous work has concluded that different WM processing information is present in the EEG/MEG and fMRI signals. Another limitation of the current paper is that although we sought reconciliation between these literatures, we conducted an fMRI but not an EEG study. The rationale for this approach was two-fold. First, the fMRI literature primarily presents stimuli at fixation rather than cueing one visual hemifield as required by the EEG/CDA literature. Second, the existing CDA literature relies on visuospatial stimulus arrays and reports a bilateral contralateral bias. We were discouraged from this approach based on our previous explorations of this possibility in two unpublished investigations using the CDA. In the first, we used a visuospatial WM task and varied set size (2-4 items) and in the second we manipulated grouping in a visuospatial WM array (set sizes 2-3). In both cases cohorts of 12-22 participants were collected and the CDA was calculated separately for left and right posterior sites. In neither case did we see a significant difference between the CDA amplitudes derived from either hemisphere. These preliminary observations are consistent with a general contralateral bias in the IPS during visuospatial WM tasks and generally consistent with our current observations. For the pure storage view to be supported, we should have observed an interaction with a significantly stronger CDA in the left hemisphere for verbal information and a significantly stronger CDA in the right hemisphere for visuospatial information. However, the possibility has been raised that various methodologies may be providing complementary information regarding function that can be challenging to reconcile, for example the fMRI/EEG/MEG study noted in the introduction (Robitaille et al., 2010).

Future work will be needed to confirm the generalizability of these findings across stimulus types. Additionally, advances in EEG source localization (Michel et al., 2004) and in paired fMRI-EEG localization studies (Cottareau, Ales, & Norcia, 2014; Kuo et al., 2014) will be helpful in supplying converging evidence with the more spatially-specific fMRI literature. Lastly, to reconcile the findings presented here, as well as to account for the discrepancies found in the current fMRI and EEG literature, and overcome under specific predictions, an updated internal attention model is needed. Thus, future work is needed that uses multiple neuroimaging methods and more standardized stimuli and stimuli presentation in order to better control for possible discrepancies.

## Acknowledgments

This work was funded by NEI R15EY022775, and NIGMS 1P20GM103650 (COBRE Project 1 Leader) to MEB. The content is solely the responsibility of the authors and does not necessarily represent the official views of the NIH, NIGMS, or NEI. We would also like to thank Dr. Gideon Caplovitz and Dr. Lars Strother for their helpful advice.

## References

- Afraz SR, Kiani R, Esteky H. Microstimulation of inferotemporal cortex influences face categorization. *Nature*. 2006; 442(7103):692–695.10.1038/nature04982 [PubMed: 16878143]
- Anderson DE, Vogel EK, Awh E. Precision in visual working memory reaches a stable plateau when individual item limits are exceeded. *The Journal of neuroscience: the official journal of the Society for Neuroscience*. 2011; 31(3):1128–1138.10.1523/JNEUROSCI.4125-10.2011 [PubMed: 21248137]
- Arcaro MJ, McMains SA, Singer BD, Kastner S. Retinotopic organization of human ventral visual cortex. *J Neurosci*. 2009; 29(34):10638–10652.10.1523/JNEUROSCI.2807-09.2009 [PubMed: 19710316]
- Argall BD, Saad ZS, Beauchamp MS. Simplified intersubject averaging on the cortical surface using SUMA. *Hum Brain Mapp*. 2006; 27(1):14–27.10.1002/hbm.20158 [PubMed: 16035046]
- Baddeley A. *Working Memory*. 1986
- Baddeley A. The episodic buffer: a new component of working memory? *Trends Cogn Sci*. 2000; 4(11):417–423. [PubMed: 11058819]
- Baddeley A. Working memory: looking back and looking forward. *Nature Reviews Neuroscience*. 2003; 4:829–839.
- Baddeley, A.; Hitch, GJ., editors. *Working memory*. Vol. 8. New York: Academic press; 1974.
- Bandettini PA, Jesmanowicz A, Wong EC, Hyde JS. Processing strategies for time-course data sets in functional MRI of the human brain. *Magnetic resonance in medicine: official journal of the Society of Magnetic Resonance in Medicine / Society of Magnetic Resonance in Medicine*. 1993; 30(2): 161–173.
- Barrouillet P, Camos V. Interference: unique source of forgetting in working memory? *Trends Cogn Sci*. 2009; 13(4):145–146. author reply 146–147. [PubMed: 19285911]
- Battelli L, Alvarez GA, Carlson T, Pascual-Leone A. The role of the parietal lobe in visual extinction studied with transcranial magnetic stimulation. *J Cogn Neurosci*. 2009; 21(10):1946–1955.10.1162/jocn.2008.21149 [PubMed: 18855545]
- Becker JT, MacAndrew DK, Fiez JA. A comment on the functional localization of the phonological storage subsystem of working memory. *Brain Cogn*. 1999; 41(1):27–38.10.1006/brcg.1999.1094 [PubMed: 10536084]
- Berryhill ME. Insights from neuropsychology: pinpointing the role of the posterior parietal cortex in episodic and working memory. *Frontiers in integrative neuroscience*. 2012; 6:31.10.3389/fnint.2012.00031 [PubMed: 22701406]
- Berryhill ME, Chein JM, Olson IR. At the intersection of attention and memory: the mechanistic role of the posterior parietal lobe in working memory. *Neuropsychologia*. 2011; 49:1306–1315.
- Brainard DH. The Psychophysics Toolbox. *Spat Vis*. 1997; 10(4):433–436. [PubMed: 9176952]
- Bray S, Almas R, Arnold AE, Iaria G, MacQueen G. Intraparietal sulcus activity and functional connectivity supporting spatial working memory manipulation. *Cereb Cortex*. 2015; 25(5):1252–1264.10.1093/cercor/bht320 [PubMed: 24275831]
- Bray S, Arnold AE, Iaria G, MacQueen G. Structural connectivity of visuotopic intraparietal sulcus. *Neuroimage*. 2013; 82:137–145.10.1016/j.neuroimage.2013.05.080 [PubMed: 23721725]
- Brighina F, Bisiach E, Piazza A, Oliveri M, La Bua V, Daniele O, Fierro B. Perceptual and response bias in visuospatial neglect due to frontal and parietal repetitive transcranial magnetic stimulation in normal subjects. *Neuroreport*. 2002; 13(18):2571–2575.10.1097/01.wnr.0000052321.62862.7e [PubMed: 12499870]

- Chein JM, Fiez JA. Evaluating models of working memory through the effects of concurrent irrelevant information. *J Exp Psychol Gen.* 2010; 139(1):117–137. doi:2010-01266-002[pii]10.1037/a0018200. [PubMed: 20121315]
- Chein JM, Moore AB, Conway AR. Domain-general mechanisms of complex working memory span. *Neuroimage.* 2011; 54(1):550–559. doi:S1053-8119(10)01059-1[pii]10.1016/j.neuroimage.2010.07.067. [PubMed: 20691275]
- Chein JM, Ravizza SM, Fiez JA. Using neuroimaging to evaluate models of working memory and their implications for language processing. *Journal of Neurolinguistics.* 2003; 16:315–339.
- Cottareau BR, Ales JM, Norcia AM. How to use fMRI functional localizers to improve EEG/MEG source estimation. *J Neurosci Methods.* 2014.10.1016/j.jneumeth.2014.07.015
- Cowan, N. An embedded-processes model of working memory. In: Miyake, A.; Shah, P., editors. *Models of working memory: mechanisms of active maintenance and executive control.* New York: Cambridge University Press; 1999. p. 62-101.
- Cowan N. The magical number 4 in short-term memory: A reconsideration of mental storage capacity. *Behavioral & Brain Sciences.* 2001; 24(1):87–114. [PubMed: 11515286]
- Cowan N. The focus of attention as observed in visual working memory tasks: Making sense of competing claims. *Neuropsychologia.* 2011; 49(6):1401–1406.10.1016/j.neuropsychologia.2011.01.035 [PubMed: 21277880]
- Cowan N, Li D, Moffitt A, Becker TM, Martin EA, Saults JS, Christ SE. A neural region of abstract working memory. *J Cogn Neurosci.* 2011; 23(10):2852–2863.10.1162/jocn.2011.21625 [PubMed: 21261453]
- Cox RW. AFNI: software for analysis and visualization of functional magnetic resonance neuroimages. *Comput Biomed Res.* 1996; 29(3):162–173. [PubMed: 8812068]
- Cutini S, Scarpa F, Scatturin P, Jolicoeur P, Pluchino P, Zorzi M, Dell'acqua R. A hemodynamic correlate of lateralized visual short-term memories. *Neuropsychologia.* 2011; 49(6):1611–1621.10.1016/j.neuropsychologia.2010.12.009 [PubMed: 21163274]
- Dale AM, Fischl B, Sereno MI. Cortical surface-based analysis. I. Segmentation and surface reconstruction. *Neuroimage.* 1999; 9(2):179–194.10.1006/nimg.1998.0395 [PubMed: 9931268]
- Drew TW, McCollough AW, Vogel EK. Event-related potential measures of visual working memory. *Clinical EEG and neuroscience: official journal of the EEG and Clinical Neuroscience Society.* 2006; 37(4):286–291.
- Dumoulin SO, Wandell BA. Population receptive field estimates in human visual cortex. *Neuroimage.* 2008; 39(2):647–660.10.1016/j.neuroimage.2007.09.034 [PubMed: 17977024]
- Engel SA, Glover GH, Wandell BA. Retinotopic organization in human visual cortex and the spatial precision of functional MRI. *Cereb Cortex.* 1997; 7(2):181–192. [PubMed: 9087826]
- Fedorenko E, Duncan J, Kanwisher N. Broad domain generality in focal regions of frontal and parietal cortex. *Proc Natl Acad Sci U S A.* 2013; 110(41):16616–16621.10.1073/pnas.1315235110 [PubMed: 24062451]
- Fierro B, Brighina F, Oliveri M, Piazza A, La Bua V, Buffa D, Bisiach E. Contralateral neglect induced by right posterior parietal rTMS in healthy subjects. *Neuroreport.* 2000; 11(7):1519–1521. [PubMed: 10841369]
- Fischl B, Sereno MI, Dale AM. Cortical surface-based analysis. II: Inflation, flattening, and a surface-based coordinate system. *Neuroimage.* 1999; 9(2):195–207.10.1006/nimg.1998.0396 [PubMed: 9931269]
- Fischl B, Sereno MI, Tootell RB, Dale AM. High-resolution intersubject averaging and a coordinate system for the cortical surface. *Hum Brain Mapp.* 1999; 8(4):272–284. [PubMed: 10619420]
- Friston KJ, Frith CD, Turner R, Frackowiak RS. Characterizing evoked hemodynamics with fMRI. *Neuroimage.* 1995; 2(2):157–165. [PubMed: 9343598]
- Gao Z, Li J, Liang J, Chen H, Yin J, Shen M. Storing fine detailed information in visual working memory--Evidence from event-related potentials. *Journal of Vision.* 2009; 9(7):17–17.10.1167/9.7.17 [PubMed: 19761332]
- Harrison SA, Tong F. Decoding reveals the contents of visual working memory in early visual areas. *Nature.* 2009; 458(7238):632–635.10.1038/nature07832 [PubMed: 19225460]

- Heilman KM, Van Den Abell T. Right hemisphere dominance for attention: the mechanism underlying hemispheric asymmetries of inattention (neglect). *Neurology*. 1980; 30(3):327–330. [PubMed: 7189037]
- Herwig U, Abler B, Schonfeldt-Lecuona C, Wunderlich A, Grothe J, Spitzer M, Walter H. Verbal storage in a premotor-parietal network: evidence from fMRI-guided magnetic stimulation. *Neuroimage*. 2003; 20(2):1032–1041.10.1016/S1053-8119(03)00368-9 [PubMed: 14568473]
- Ikkai A, McCollough AW, Vogel E. Contralateral delay activity provides a neural measure of the number of representations in visual working memory. *J Neurophysiol*. 2010; 103:1963–1968. doi: 00978.2009[pii]10.1152/jn.00978.2009. [PubMed: 20147415]
- Jolicoeur P, Brisson B, Robitaille N. Dissociation of the N2pc and sustained posterior contralateral negativity in a choice response task. *Brain Research*. 2008; 1215:160–172.10.1016/j.brainres.2008.03.059 [PubMed: 18482718]
- Kinsbourne M. Hemi-neglect and hemisphere rivalry. *Adv Neurol*. 1977; 18:41–49. [PubMed: 920524]
- Kiyonaga A, Egner T. Working memory as internal attention: toward an integrative account of internal and external selection processes. *Psychon Bull Rev*. 2013; 20(2):228–242.10.3758/s13423-012-0359-y [PubMed: 23233157]
- Klaver P, Talsma D, Wijers AA, Heinze HJ, Mulder G. An event-related brain potential correlate of visual short-term memory. *Neuroreport*. 1999; 10(10):2001–2005. [PubMed: 10424664]
- Konen CS, Kastner S. Representation of eye movements and stimulus motion in topographically organized areas of human posterior parietal cortex. *J Neurosci*. 2008; 28(33):8361–8375.10.1523/JNEUROSCI.1930-08.2008 [PubMed: 18701699]
- Kuo CC, Luu P, Morgan KK, Dow M, Davey C, Song J, et al. Tucker DM. Localizing movement-related primary sensorimotor cortices with multi-band EEG frequency changes and functional MRI. *PLoS ONE*. 2014; 9(11):e112103.10.1371/journal.pone.0112103 [PubMed: 25375957]
- Langel J, Hakun J, Zhu DC, Ravizza SM. Functional specialization of the left ventral parietal cortex in working memory. *Front Hum Neurosci*. 2014; 8:440.10.3389/fnhum.2014.00440 [PubMed: 24994977]
- Lewandowsky S, Oberauer K, Brown GDA. No temporal decay in verbal short-term memory. *Trends in Cognitive Sciences*. 2009; 13(3):120–126.10.1016/j.tics.2008.12.003 [PubMed: 19223224]
- Li D, Christ SE, Cowan N. Domain-general and domain-specific functional networks in working memory. *Neuroimage*. 2014; 102P2:646–656.10.1016/j.neuroimage.2014.08.028 [PubMed: 25178986]
- Majerus S, Bastin C, Poncelet M, Van der Linden M, Salmon E, Collette F, Maquet P. Short-term memory and the left intraparietal sulcus: focus of attention? Further evidence from a face short-term memory paradigm. *Neuroimage*. 2007; 35(1):353–367. [PubMed: 17240164]
- Majerus S, Cowan N, Peters F, Van Calster L, Phillips C, Schrouff J. Cross-Modal Decoding of Neural Patterns Associated with Working Memory: Evidence for Attention-Based Accounts of Working Memory. *Cereb Cortex*. 2014; 10.1093/cercor/bhu189
- Majerus S, Poncelet M, Van der Linden M, Albouy G, Salmon E, Sterpenich V, et al. Maquet P. The left intraparietal sulcus and verbal short-term memory: focus of attention or serial order? *Neuroimage*. 2006; 32(2):880–891. [PubMed: 16702002]
- McCollough AW, Machizawa MG, Vogel EK. Electrophysiological measures of maintaining representations in visual working memory. *Cortex; a journal devoted to the study of the nervous system and behavior*. 2007; 43(1):77–94.
- Mesulam MM. A cortical network for directed attention and unilateral neglect. *Annals of neurology*. 1981; 10(4):309–325.10.1002/ana.410100402 [PubMed: 7032417]
- Michel CM, Murray MM, Lantz G, Gonzalez S, Spinelli L, Grave de Peralta R. EEG source imaging. *Clin Neurophysiol*. 2004; 115(10):2195–2222.10.1016/j.clinph.2004.06.001 [PubMed: 15351361]
- Mitchell DJ, Cusack R. Flexible, Capacity-Limited Activity of Posterior Parietal Cortex in Perceptual as well as Visual Short-Term Memory Tasks. *Cerebral Cortex*. 2007; 18(8):1788–1798.10.1093/cercor/bhm205 [PubMed: 18042643]

- Mitchell DJ, Cusack R. The temporal evolution of electromagnetic markers sensitive to the capacity limits of visual short-term memory. *Front Hum Neurosci.* 2011; 5:18.10.3389/fnhum.2011.00018 [PubMed: 21415910]
- Mruczek RE, von Loga IS, Kastner S. The representation of tool and non-tool object information in the human intraparietal sulcus. *J Neurophysiol.* 2013; 109(12):2883–2896.10.1152/jn.00658.2012 [PubMed: 23536716]
- Olson IR, Berryhill ME. Some surprising findings on the involvement of the parietal lobe in human memory. *Neurobiol Learn Mem.* 2009; 91:155–165. [PubMed: 18848635]
- Palva JM, Monto S, Kulashekhar S, Palva S. Neuronal synchrony reveals working memory networks and predicts individual memory capacity. *Proc Natl Acad Sci U S A.* 2010; 107(16):7580–7585.10.1073/pnas.0913113107 [PubMed: 20368447]
- Pinsk MA, DeSimone K, Moore T, Gross CG, Kastner S. Representations of faces and body parts in macaque temporal cortex: a functional MRI study. *Proc Natl Acad Sci U S A.* 2005; 102(19):6996–7001.10.1073/pnas.0502605102 [PubMed: 15860578]
- Plow EB, Cattaneo Z, Carlson TA, Alvarez GA, Pascual-Leone A, Battelli L. The compensatory dynamic of inter-hemispheric interactions in visuospatial attention revealed using rTMS and fMRI. *Front Hum Neurosci.* 2014; 8:226.10.3389/fnhum.2014.00226 [PubMed: 24860462]
- Pourtois G, Vandermereen Y, Olivier E, de Gelder B. Event-related TMS over the right posterior parietal cortex induces ipsilateral visuo-spatial interference. *Neuroreport.* 2001; 12(11):2369–2374. [PubMed: 11496112]
- Ravizza S, Delgado M, Chein J, Becker J, Fiez J. Functional dissociations within the inferior parietal cortex in verbal working memory. *Neuroimage.* 2004; 22(2):562–573.10.1016/j.neuroimage.2004.01.039 [PubMed: 15193584]
- Repovs G, Baddeley A. The multi-component model of working memory: Explorations in experimental cognitive psychology. *Neuroscience.* 2006; 139(1):5–21. [PubMed: 16517088]
- Robitaille N, Marois R, Todd J, Grimault S, Cheyne D, Jolicoeur P. Distinguishing between lateralized and nonlateralized brain activity associated with visual short-term memory: fMRI, MEG, and EEG evidence from the same observers. *Neuroimage.* 2010; 53(4):1334–1345.10.1016/j.neuroimage.2010.07.027 [PubMed: 20643214]
- Rottschy C, Langner R, Dogan I, Reetz K, Laird AR, Schulz JB, et al. Eickhoff SB. Modelling neural correlates of working memory: a coordinate-based meta-analysis. *Neuroimage.* 2012; 60(1):830–846.10.1016/j.neuroimage.2011.11.050 [PubMed: 22178808]
- Saad Z, Reynolds R, Cox RJ, Argall B, Japee S. SUMA: an interface for surface-based intra- and inter-subject analysis. *PROC ISBI.* 2004; 2:1510–1511.
- Schluppeck D, Glimcher P, Heeger DJ. Topographic organization for delayed saccades in human posterior parietal cortex. *J Neurophysiol.* 2005; 94(2):1372–1384.10.1152/jn.01290.2004 [PubMed: 15817644]
- Serences JT, Ester EF, Vogel EK, Awh E. Stimulus-specific delay activity in human primary visual cortex. *Psychol Sci.* 2009; 20(2):207–214. doi:PSCI2276[pil]10.1111/j.1467-9280.2009.02276.x. [PubMed: 19170936]
- Sereno MI, Dale AM, Reppas JB, Kwong KK, Belliveau JW, Brady TJ, et al. Tootell RB. Borders of multiple visual areas in humans revealed by functional magnetic resonance imaging. *Science.* 1995; 268(5212):889–893. [PubMed: 7754376]
- Sereno MI, Pitzalis S, Martinez A. Mapping of contralateral space in retinotopic coordinates by a parietal cortical area in humans. *Science.* 2001; 294(5545):1350–1354.10.1126/science.1063695 [PubMed: 11701930]
- Sheremata SL, Bettencourt KC, Somers DC. Hemispheric asymmetry in visuotopic posterior parietal cortex emerges with visual short-term memory load. *The Journal of neuroscience: the official journal of the Society for Neuroscience.* 2010; 30(38):12581–12588.10.1523/JNEUROSCI.2689-10.2010 [PubMed: 20861364]
- Sheremata SL, Silver MA. Hemisphere-dependent attentional modulation of human parietal visual field representations. *J Neurosci.* 2015; 35(2):508–517.10.1523/JNEUROSCI.2378-14.2015 [PubMed: 25589746]

- Silver MA, Kastner S. Topographic maps in human frontal and parietal cortex. *Trends Cogn Sci.* 2009; 13(11):488–495.10.1016/j.tics.2009.08.005 [PubMed: 19758835]
- Silver MA, Ress D, Heeger DJ. Topographic maps of visual spatial attention in human parietal cortex. *J Neurophysiol.* 2005; 94(2):1358–1371.10.1152/jn.01316.2004 [PubMed: 15817643]
- Song JH, Jiang Y. Visual working memory for simple and complex features: an fMRI study. *Neuroimage.* 2006; 30(3):963–972. [PubMed: 16300970]
- Sprague TC, Serences JT. Attention modulates spatial priority maps in the human occipital, parietal and frontal cortices. *Nat Neurosci.* 2013; 16(12):1879–1887.10.1038/nn.3574 [PubMed: 24212672]
- Swisher JD, Halko MA, Merabet LB, McMains SA, Somers DC. Visual topography of human intraparietal sulcus. *J Neurosci.* 2007; 27(20):5326–5337.10.1523/JNEUROSCI.0991-07.2007 [PubMed: 17507555]
- Szczepanski SM, Kastner S. Shifting attentional priorities: control of spatial attention through hemispheric competition. *The Journal of neuroscience: the official journal of the Society for Neuroscience.* 2013; 33(12):5411–5421.10.1523/JNEUROSCI.4089-12.2013 [PubMed: 23516306]
- Szczepanski SM, Konen CS, Kastner S. Mechanisms of spatial attention control in frontal and parietal cortex. *The Journal of neuroscience: the official journal of the Society for Neuroscience.* 2010; 30(1):148–160.10.1523/JNEUROSCI.3862-09.2010 [PubMed: 20053897]
- Talairach, J.; Tournoux, P. Co-planar stereotaxic atlas of the human brain. New York: Thieme; 1988.
- Todd JJ, Marois R. Capacity limit of visual short-term memory in human posterior parietal cortex. *Nature.* 2004; 428(6984):751–754. [PubMed: 15085133]
- Todd JJ, Marois R. Posterior parietal cortex activity predicts individual differences in visual short-term memory capacity. *Cogn Affect Behav Neurosci.* 2005; 5(2):144–155. [PubMed: 16180621]
- Trapp S, Lepsien J. Attentional orienting to mnemonic representations: reduction of load-sensitive maintenance-related activity in the intraparietal sulcus. *Neuropsychologia.* 2012; 50(12):2805–2811.10.1016/j.neuropsychologia.2012.08.003 [PubMed: 22960415]
- Unsworth N, Engle RW. The nature of individual differences in working memory capacity: active maintenance in primary memory and controlled search from secondary memory. *Psychol Rev.* 2007; 114(1):104–132. [PubMed: 17227183]
- Vilberg KL, Rugg MD. Memory retrieval and the parietal cortex: a review of evidence from a dual-process perspective. *Neuropsychologia.* 2008; 46(7):1787–1799. [PubMed: 18343462]
- Vogel EK, Machizawa MG. Neural activity predicts individual differences in visual working memory capacity. *Nature.* 2004; 428(6984):748–751. [PubMed: 15085132]
- Vogel EK, McCollough AW, Machizawa MG. Neural measures reveal individual differences in controlling access to working memory. *Nature.* 2005; 438(7067):500–503. doi:nature04171[pil]10.1038/nature04171. [PubMed: 16306992]
- Wang L, Mruczek RE, Arcaro MJ, Kastner S. Probabilistic Maps of Visual Topography in Human Cortex. *Cereb Cortex.* 2014.10.1093/cercor/bhu277
- Xu Y. The role of the superior intraparietal sulcus in supporting visual short-term memory for multifeature objects. *J Neurosci.* 2007; 27(43):11676–11686. [PubMed: 17959810]
- Xu Y, Chun MM. Dissociable neural mechanisms supporting visual short-term memory for objects. *Nature.* 2006; 440(7080):91–95.10.1038/nature04262 [PubMed: 16382240]
- Yarkoni T, Poldrack RA, Van Essen DC, Wager TD. Cognitive neuroscience 2.0: building a cumulative science of human brain function. *Trends Cogn Sci.* 2010; 14(11):489–496.10.1016/j.tics.2010.08.004 [PubMed: 20884276]

### Research Highlights

- In this study we compare two theoretical accounts of working memory.
- We studied parietal contributions to visuospatial and verbal working memory.
- There was a contralateral bias along the intraparietal sulci across stimulus type.
- Stronger biases existed followed a verbal/left and visuospatial/right pattern.

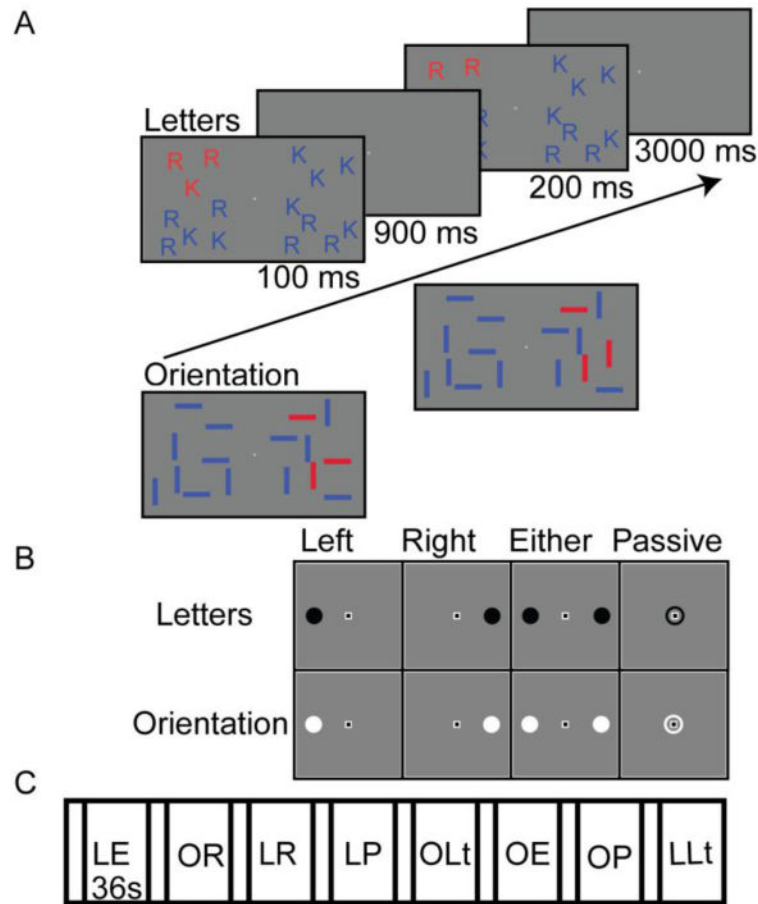


**Figure 1.** Experimental task design and block sequence. **A.** Trial sequence. Participants maintained fixation throughout the session. Stimuli were briefly presented and after a delay a probe screen appeared. Participants indicated whether the array was the same or different from the original array. An example of a letter trial is shown in the sequence and example oriented bar stimuli and a probe screen are shown below the arrow. **B.** The black cues indicated letter stimuli and the white cues indicated orientation blocks. The location of the cue indicated which hemifield should be attended. **C.** Example block sequence reflecting the various conditions. The block order was randomized for each run. Each block lasted 36 s with a 4 s inter-block interval. Abbreviations: E = either, L = letters, Lt = left, O = oriented bars, P = passive, R = right.



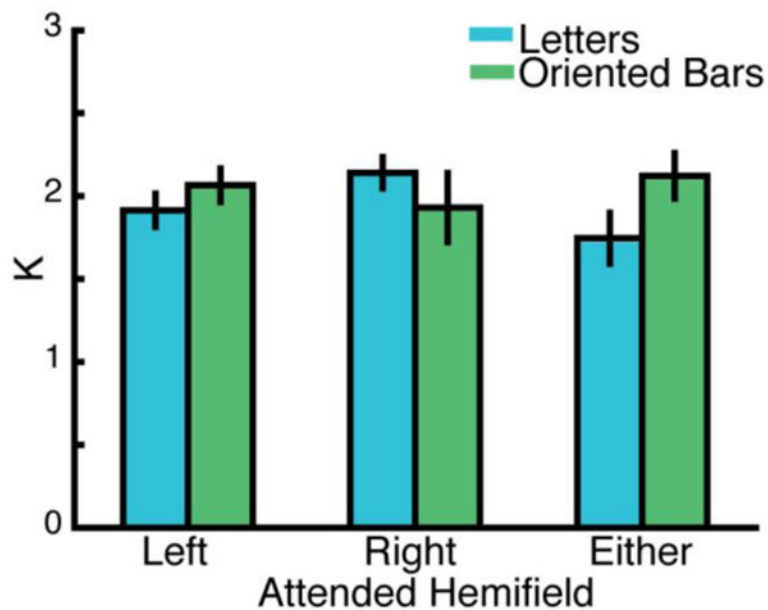


**Figure 2.** Behavioral performance reflecting the WM capacity (Cowan's K) for each stimulus type (letters, oriented bars) and for the attended hemifield at encoding (left, right, either). The bars represent the mean Cowan's K values across participants and error bars reflect the standard error of the mean. There were no significant main effects or interactions of stimulus type or hemifield, although a nonsignificant numerical trend showing stronger performance for the letter stimuli shown in the right hemifield and for the oriented bars in the left hemifield was evident.

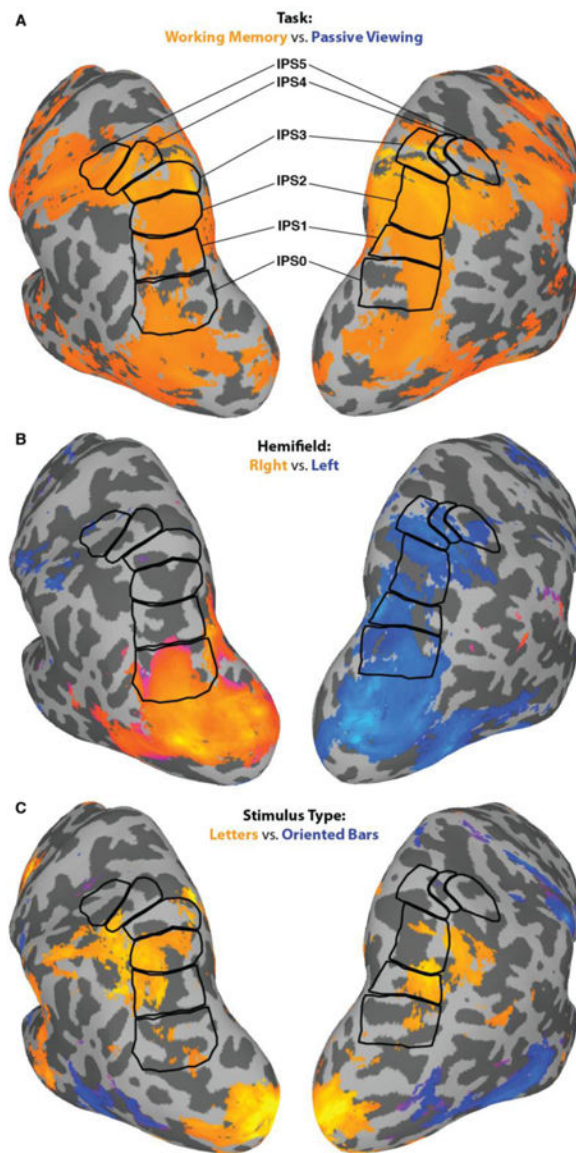


### Figure 3. Whole Brain Analyses

**A)** WM-related activity along the IPS derived from group-level analysis and presented on a cortical model of one of the participants. The WM-related activity was defined as *any* WM condition (left, right, either) > passive viewing, ( $p < .005$ , uncorrected). This image clarifies that WM-related activity was well-captured by the IPS ROIs (outlined in black) used in subsequent analyses. **B)** The contrast between stimulus hemifield (right > left;  $p < .05$ , uncorrected). This figure reveals a contralateral bias in topographic ROIs. **C)** The contrast of stimulus type (verbal > visuospatial;  $p < .05$ , uncorrected) reveals some stimulus-based differences, but no pattern of left hemisphere-verbal, right hemisphere-visuospatial, as would be predicted by a pure storage model. Whole brain activity is based on statistical maps calculated using a mixed-effects meta-analysis.

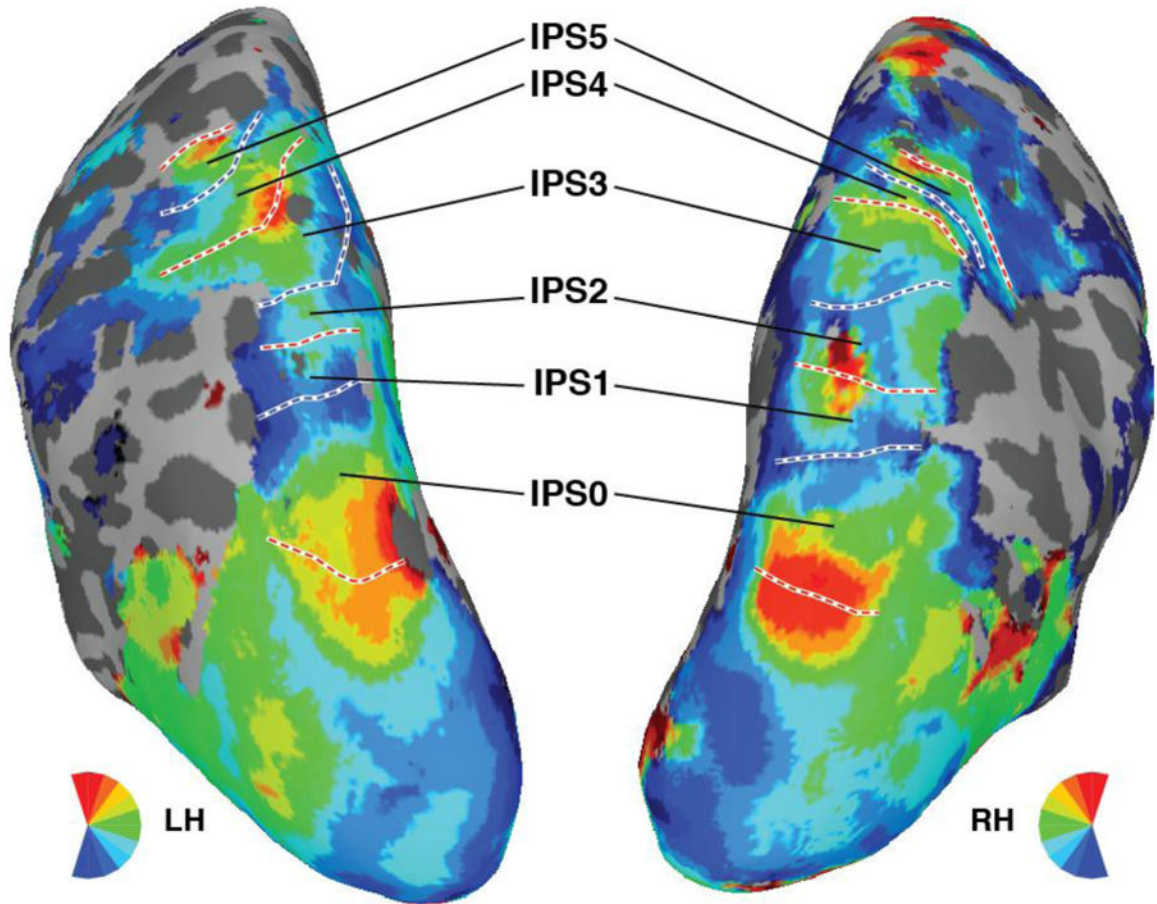


**Figure 4.** Polar angle maps and IPS ROIs delineated for one representative participant. The color code indicates the region of the visual field to which each surface node responded maximally during the retinotopic mapping session. White lines denote the ROI boundaries formed by phase reversals at, or close to, the upper vertical (dashed red) or lower vertical (dashed blue) meridians.

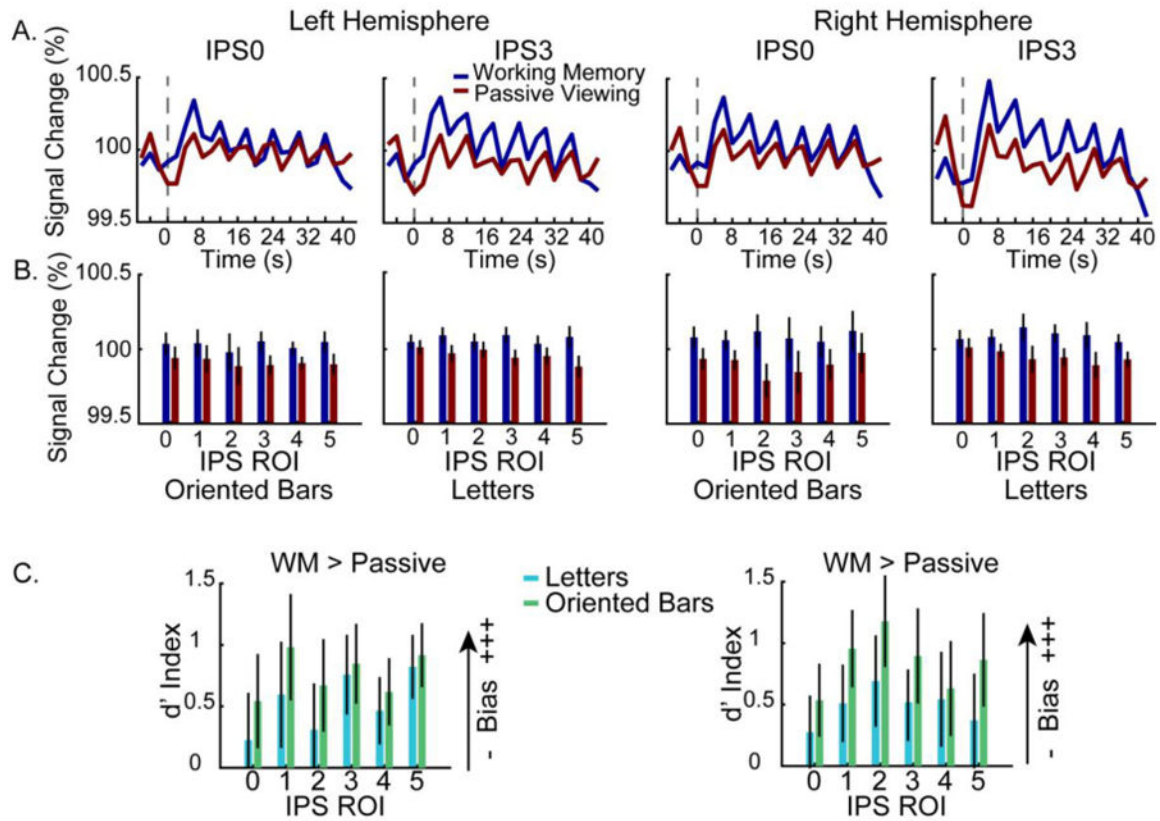


**Figure 5.**

Greater WM activity compared to passive viewing. **A.** Group-averaged timecourses reveal that throughout a trial block there was greater WM related activity compared to passive viewing in both hemispheres (left hemisphere on the left, right hemisphere on the right) for two representative IPS ROIs (IPS0 and IPS3). **B.** Average BOLD percent signal change for the WM and passive viewing conditions for all IPS ROIs. Across left and right IPS ROIs the WM task (attend to either hemifield condition) bars show greater activity than passive viewing condition. For each hemisphere, the activity associated with each stimulus type (left panels: oriented bars, right panels: letters) is shown separately. Mean BOLD signal was averaged across each block (2-40 s). Error bars represent the standard error of the mean. **C.** Greater WM activity is evident across hemispheres, ROIs, and stimulus types using the  $d'$  index. Plots of the  $d'$  weighted activation reflect a WM bias if it is greater than 0, with higher values indicating a greater WM > passive viewing bias. In all panels, data are drawn from the top 50 voxels from each ROI from the contrast of either WM condition vs. baseline. Error bars represent the standard error of the mean.

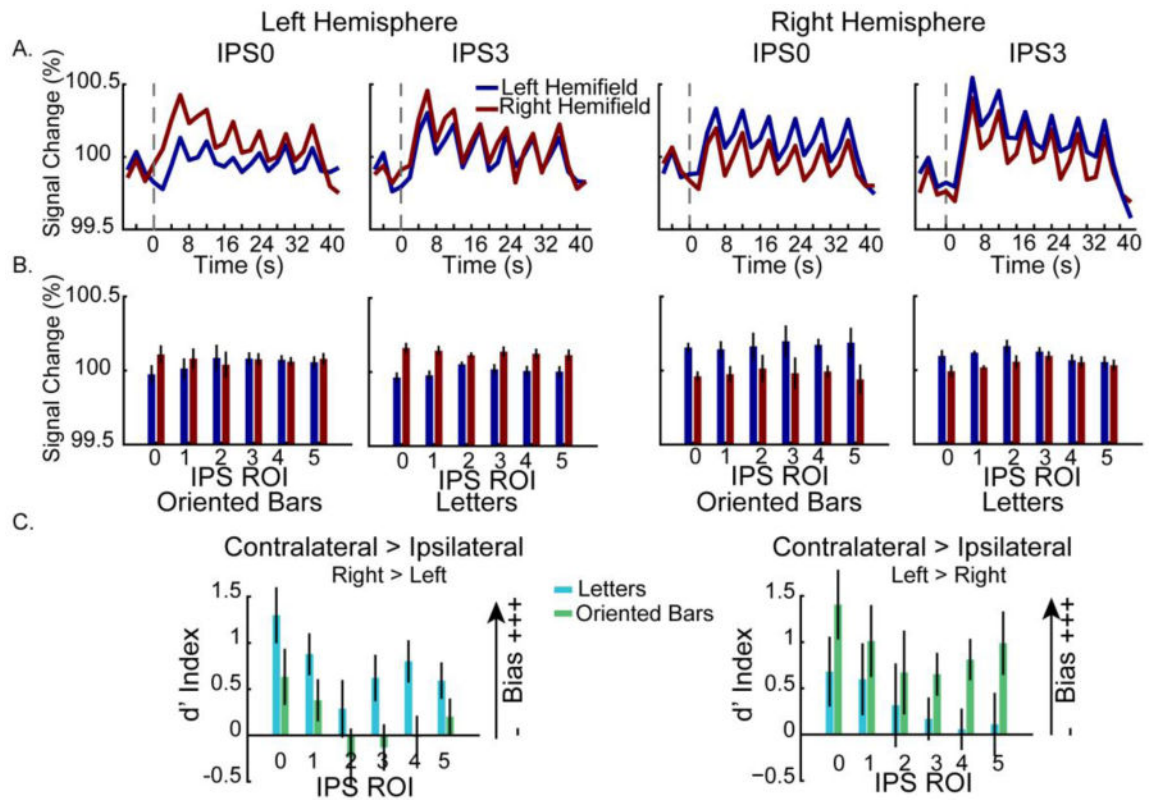


**Figure 6.**

Contralateral bias during WM is evident across left and right hemispheres. **A.** Group-averaged timecourse data reveal greater contralateral activity in two representative IPS ROIS (IPS0 and IPS3). **B.** Contralateral bias as a function of ROI, hemisphere and stimulus type (oriented bars, left panels; letters, right panels). The mean BOLD signal was averaged across each block (2-40 s). Error bars represent standard error of the mean. **C.** The contralateral bias as shown by the  $d'$  index. The  $d'$  prime index is a measure used to directly compare the mean response across conditions and is positive when there is a contralateral bias and negative when there is an ipsilateral bias, with larger values indicating greater differences across contralateral and ipsilateral WM trials. In all panels, data are drawn from the top 50 voxels from each ROI from the contrast of either WM condition vs. baseline. Error bars represent standard error of the mean.

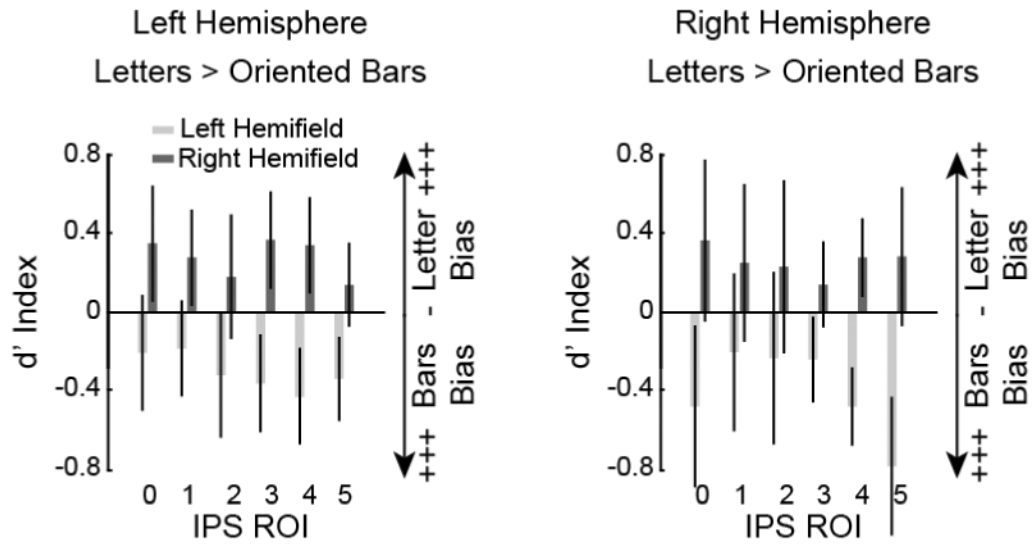


**Figure 7.**

Direct assessment of stimulus-based bias as a function of hemisphere and hemifield. These data show the contrast of stimulus types (letters vs. oriented bars) across left and right hemispheres and visual hemifields using the  $d'$  index. The  $d'$  prime index is a measure used to directly compare the mean response across stimulus types. It is positive when there is stronger activation for letter stimuli and negative when there is stronger activation for oriented bar stimuli, a value of 0 indicates no stimulus-based bias. The visuospatial oriented bar stimuli led to stronger activation across all IPS ROIs when the task was performed in the left visual hemifield (light gray bars, both panels). The verbal letter stimuli led to stronger activation when the task was performed in the right visual hemifield (dark gray bars, both panels). Data are drawn from the top 50 voxels from each ROI from the contrast of either WM condition vs. baseline. Error bars represent standard error of the mean.

**Table 1**

Talairach coordinates for topographic IPS ROIs.

ROI	HS	x	y	z
IPS0	LH	-24.7 ± 1.1	-71.7 ± 1.5	20 ± 1.3
	RH	25.7 ± 1.1	-71.6 ± 1.3	21 ± 1.2
IPS1	LH	-21.4 ± 1.4	-66.4 ± 2.5	30.3 ± 1.5
	RH	23.7 ± 1.0	-66.1 ± 2.2	33.3 ± 1.1
IPS2	LH	-18.5 ± 1.5	-63.7 ± 2.7	39.1 ± 1.6
	RH	21.1 ± 0.9	-60.7 ± 2.1	40.9 ± 0.9
IPS3	LH	-20.2 ± 1.5	-60.2 ± 2.6	45.1 ± 1.6
	RH	19.9 ± 1.3	-57.9 ± 2.1	49.2 ± 1.5
IPS4	LH	-25.2 ± 2.1	-53.2 ± 2.0	46.5 ± 2.2
	RH	25.8 ± 1.8	-55 ± 1.7	48.1 ± 1.8
IPS5	LH	-30.5 ± 1.9	-50.2 ± 2.7	48 ± 2.0
	RH	33.6 ± 2.0	-47.5 ± 1.5	48.4 ± 2.1

Mean coordinates ± SEM. HS = hemisphere, LH = left hemisphere, RH = right hemisphere.